Calibration of the WSR-88D Precipitation Processing Subsystem

EMMANOUIL N. ANAGNOSTOU* AND WITOLD F. KRAJEWSKI

Iowa Institute of Hydraulic Research, University of Iowa, Iowa City, Iowa

(Manuscript received 6 March 1997, in final form 10 February 1998)

ABSTRACT

The WSR-88D Precipitation Processing Subsystem (PPS) is a multicomponent rainfall-estimation algorithm with a large number of parameters controlling its performance. Currently, the parameter values of the PPS are set based on limited experimental studies and do not account for rainfall-regime differences. This translates into potential increase of uncertainty in the system-estimated precipitation products.

The authors propose to formulate the PPS calibration as a global optimization problem. The parameter values are determined by optimizing a selected criterion at the level of gridded hourly rainfall-accumulation products. The criterion is the root-mean-square difference between the hourly radar rainfall products and rainfall accumulations from rain gauges under the radar umbrella. The main advantages of this approach are 1) it simultaneously estimates the optimal parameters providing an integral assessment of the algorithm's performance, and 2) it allows for an assessment of the relative importance of the PPS parameters in the full context of rainfall estimation.

The optimization approach is illustrated using two months of Melbourne, Florida, WSR-88D radar-reflectivity data and the corresponding rain gauge measurements. Global optimization of the PPS parameters yields a reduction of 10% on average and up to 22% on individual days with respect to the default system. The illustration is completed by a sensitivity analysis of the PPS to identify the most significant parameters.

1. Introduction

The WSR-88D Precipitation Processing Subsystem (PPS) is designed to provide nationwide real-time quantitative estimates of precipitation with high spatial and temporal resolution. The system converts reflectivity data collected by the WSR-88D radars into rainfall accumulations. The PPS products have spatial resolution from 2 km $\times$ 1° to approximately 4 km $\times$ 4 km, and temporal resolution from 5 min (scan-to-scan products) to several hours (Klazura and Imy 1993). The PPS rainfall estimates are input to several hydrometeorological and water resources applications, including hydrologic forecasting, water resource management, and operation and control of water system (Hudlow 1984; Smith et al. 1992; NRC 1994). For this reason, the PPS products have attracted the attention of many practicing hydrologists and engineers. Several studies report the use of WSR-88D products in hydrology (James et al. 1993; Smith et al. 1996).

The PPS consists of several interconnected components representing a multistage radar rainfall estimation process. The subjectively determined functions used to describe the internal operations of the processing stages were designed over a decade ago. These functions were first described in Ahnert et al. (1983) and Hudlow (1988); most recent descriptions are given by Hunter (1996) and Fulton et al. (1998). The nonlinearity of the functions and the number of parameters used by the PPS to represent the rainfall estimation process clearly imply the complexity of this system. For the PPS to perform at a high level and provide accurate rainfall estimates, it is necessary to use the proper parameter values that control its processing functions. We will use the term ''system calibration'' to refer to the process of selecting the parameter values for the PPS.

The default PPS parameters are based on quantitative research dating back to the Global Atmospheric Research Program Atlantic Tropical Experiment (Hudlow et al. 1979). The same parameter values were originally used at all WSR-88D radar sites, despite regional and seasonal variability of the local rainfall processes. Some of the default parameter values disengage certain PPS components—this is done because determination of ''good'' values for these parameters is difficult and should not be done ad hoc. Recent operational experience and research at the National Weather Service (NWS) have led to changes of some of these parameters at several WSR-88D sites. However, lack of thorough

* Current affiliation: Universities Space Research Association, NASA/Goddard Space Flight Center, Greenbelt, Maryland.

Corresponding author address: Dr. Witold F. Krajewski, The University of Iowa, Institute of Hydraulic Research, College of Engineering, 404 Hydraulics Laboratory, Iowa City, IA 52242-1585.
E-mail: witold-krajewski@uiowa.edu

data-based studies limits our knowledge of the behavior of the PPS and the sensitivity of the system with respect to parameter changes. This points to the operational need for a robust mechanism to determine optimal parameter values for the PPS (Smith and Krajewski 1994).

This study has two objectives. First, we present a framework for calibration of real-time radar rainfall estimation algorithms. The proposed framework is used to determine the best parameter values of the PPS using a two-month period of WSR-88D radar and rain gauge data from Melbourne, Florida (KMLB). Second, we investigate the sensitivity of the PPS with respect to deviations of the parameters from their optimal values. We show that some of the parameters significantly affect the system's performance, while others play an insignificant role.

The proposed framework builds on the work of Ciach et al. (1997), which provides a methodology for global optimization of a multicomponent radar rainfall algorithm. The main argument for using a calibration procedure that optimizes the system performance at the final products level is as follows: because of the complex and nonlinear processes involved in radar rainfall measurement and estimation, optimization of each component separately does not assure optimal overall performance of the system at the final stage. To provide user with best rainfall products, the performance requirements should be applied at the product level (i.e., resolution).

In this paper our focus is on hourly rainfall fields gridded using the Hydrologic Rainfall Analysis Project (HRAP) grid definition (approximately 4 km $\times$ 4 km). We propose an automatic calibration to determine optimal values of the PPS parameters. The optimality criterion is minimization of the root-mean-square difference between the hourly rainfall accumulation estimated using the PPS and observed by rain gauges.

Numerous studies report automatic calibration procedures for multicomponent hydrologic systems and models (Hendrickson et al. 1988; Gan and Burges 1990, among others). Although these studies focused on calibration of conceptual rainfall–runoff models, their methodologies can be applied to calibration of radar rainfall algorithms. The above studies report that uncertainties inherent in the data and highly nonlinear structures of the involved functions can cause difficulties in finding unique solutions. Given the type of errors in radar rainfall data (see Austin 1987; Zawadzki 1984) and the nonlinear nature of the radar rainfall algorithms, one should expect similar radar rainfall calibration problems. We adopted a recently developed automated global optimization method by Duan et al. (1993) that is capable of dealing with such difficulties.

We test the proposed calibration scheme using an extensive dataset of volume scan reflectivity observations and rain gauge rainfall measurements. The data are from the KMLB site and span the period of two months: 3 August–30 September 1995. This dataset, although extensive in size, represents only one season at a single site. Thus, fundamental issues such as geographic and climatological variations and stability of the derived parameters are not addressed here.

The organization of this paper is as follows. A short description of the PPS is given in section 2. The formulation of the calibration problem is discussed in section 3. Section 4 provides a short review of the existing automatic optimization methods and a short description of the selected method; in section 5 we present the study region and the data; in section 6 the optimal parameters of the PPS based on the two-month period of actual data; in section 7 we discuss the sensitivity analysis results and we offer conclusions in section 8.

2. Precipitation processing subsystem

The PPS is a multicomponent radar rainfall-estimation algorithm. The purpose of this algorithm is to convert the WSR-88D radar reflectivity data producing rainfall accumulation maps for different duration. The four processing steps of the PPS are 1) precipitation preprocessing, to obtain the best reflectivity field; 2) precipitation rate, to convert reflectivity-to-rainfall rate; 3) precipitation accumulation, to construct rainfall maps; and 4) precipitation adjustment, to ensure consistence with rain gauge observations. A summary of the processes and parameters involved in each step is provided below.

Precipitation preprocessing involves basic quality control procedures applied to reflectivities from the lowest four scans. These procedures include corrections for beam blocking effect and spurious echoes due to outliers and ground returns. Beam blocking effect is important when radar is located in hilly terrain or within a city. To avoid ground clutter contamination at close range ($<$40 km) the two upper scans are used in rainfall estimation. Between 40 and 150 km (both adaptable) a continuity test takes place to decide whether the lowest scan is contaminated by ground returns. The continuity test is based on the fraction of echo area eliminated from the lowest to the next tilt scan. Whenever this fraction exceeds a specific threshold the lowest scan is excluded from the calculations. Subsequently, an outlier correction procedure is applied. Procedure 1 sets isolated values ($>Z_{\min}$) to zero dBZ if less than two of its neighboring bins are greater than $Z_{\min}$, and 2 replaces extreme values ($>Z_{\max}$) with a small value (Z_{tlt}) if there are neighboring values greater than $Z_{\max}$; otherwise the average of the neighboring values is used. Finally, a hybrid reflectivity scan is assembled from the lowest four scans. The elevation to be used at each range and azimuth is defined by a site-specific hybrid scan adaptation file generated off-line at the Operational Support Facility of the NWS. At far ranges (defined by the biscan minimum range parameter, R_{bi}) the PPS chooses the largest reflectivity value from the lowest two scans.

The precipitation rate processing step involves con-

TABLE 1. NEXRAD-PPS investigated parameters' symbols, default values, and description. The values in the parentheses correspond to the tropical *Z–R* relationship.

Symbol	Default value	PPS function	Description
Z_{min}	18 dB*Z*	Preprocessing	Used in test for spurious noise and nonprecipitating isolated reflectivities.
Z_{max}	53 dB*Z*	Preprocessing	Used in test for precipitating outliers
Z_{dt}	7 dB*Z*	Preprocessing	Value reflectivity outlier is corrected if any of the surrounding neighbor values are also $>Z_{max}$
R_{bi}	180 km	Preprocessing	Minimum range for which biscan maximization is applied
j_{co}	230 km	Precipitation rate	Range beyond which range correction is applied
CO1	0.0	Precipitation rate	Coefficient in range correction equation
CO2	1.0	Precipitation rate	Coefficient in range correction equation
CO3	0.0	Precipitation rate	Coefficient in range correction equation
min (*Z* to*R*)	0 dB*Z*	Precipitation rate	Minimum reflectivity converted to rainrate
max (*Z* to *R*)	53 dB*Z*	Precipitation rate	Maximum reflectivity converted to rainrate
A	300 (250)	Precipitation rate	Coefficient in *Z–R* relation
B	1.4 (1.2)	Precipitation rate	Exponential power in *Z–R* relation

version of the hybrid reflectivity map to a rainfall-rate map. This is done with the use of a power law *Z–R* relationship. The reflectivity values used in the *Z–R* relationship are truncated at an upper-reflectivity threshold (max *Z* to *R*) to account for hail contamination effects. Also, reflectivity values lower than a lower-reflectivity threshold (min *Z* to *R*) are assigned zero rainfall rate. A temporal continuity test, which examines the increase/decrease of total field accumulated water between two sequential scans, is conducted next. Subsequently, range effect correction is applied based on the following formula:

$$\mathrm{dB}R_{\mathrm{cor}}(i, j) = \mathrm{CO1} + \mathrm{CO2}\ \mathrm{dB}R(i, j) + \mathrm{CO3}\ \log_{10}[r(i, j)] \quad \text{if } j > j_{\mathrm{co}}, \tag{1}$$

where dB*R* and dBR_{cor} are the before and after range correction rainfall rates [$\log_{10}$ (mm h^{-1})] of the *i*th azimuth and *j*th range radar cell; *r* is the (*i*, *j*) cell's distance from the radar; j_{co} is the cutoff radar range parameter beyond which the range dependence correction formula is applied; and CO1, CO2, and CO3 are the range correction formula parameters. This correction has not been applied in any operational WSR-88D to date.

The third processing step includes production of rainfall accumulation maps for different durations (1 h, 3 h, storm total, or operator defined). The rainfall maps are transformed from polar coordinates to the HRAP grid, which is a function of latitude and approximately 4 km × 4 km within the United States (Fulton et al. 1998).

The final processing step involves mean-field bias correction from 1 h gauge data applied to the gridded 1 h rainfall maps (Smith and Krajewski 1991; Anagnostou et al. 1998a). The current operational version of the PPS runs with the bias correction deactivated. For an elaborate discussion on the processing steps of the PPS, particularly the background and intent of each, the reader is referred to Hunter (1996) and Fulton et al. (1998).

3. Formulation of the PPS calibration problem

It is a traditional belief that performance of radar rainfall-estimation algorithms is mainly determined by a proper choice of the radar reflectivity–rainfall rate (*Z–R*) relationship. There are many studies in the literature reporting regression-based *Z–R* parameters from a limited number of storms; a large number of these parameters is listed in Battan (1973) and Doviak and Zrnic (1992). Although the important role of *Z–R* choice is undeniable, there are many other elements of radar rainfall-estimation systems that significantly affect their performance. For the PPS, *Z–R* represents only one component of the processing system. As discussed in section 2, the algorithm has four processing steps. The main parameters that control the different functions along with their originally proposed default values are shown in Table 1. From the above it is clear that rainfall estimation for PPS is more than just a *Z–R* transformation.

Calibration of multicomponent algorithms, such as the PPS, involves two characteristic features: 1) definition of the error to represent the discrepancy between the system's estimates and ''true'' rainfall, and 2) formulation of a performance criterion (or objective func-

tion) in terms of some sample statistics of the error and the system parameters. The algorithm parameters are estimated by minimizing this objective function.

The objective function in this study is defined as the root-mean-square (rms) difference between radar and rain gauge hourly accumulations:

$$\mathrm{rms}(\boldsymbol{\Theta}) = \left\langle \frac{1}{N_p N_g} \sum_{i=1}^{N_p} \sum_{j=1}^{N_g} \{[R_g(i, j) - R_r(\boldsymbol{\Theta}, i, j)]^2\} \right\rangle^{1/2}, \quad (2)$$

where R_g is the hourly rainfall accumulation from rain gauge measurement and R_r is the corresponding mean-areal hourly radar rainfall product at the ith time period, jth rain gauge location (HRAP pixel), and for the vector $\boldsymbol{\theta} = (\theta_1, \theta_2, \theta_3, \ldots, \theta_k)$ of the parameter values. Here, N_p and N_g are the number of hourly time periods and rain gauge–radar pairs, respectively, in the calibration data sample.

The objective function operates at the final (1 h) rainfall products level. The minimum of this objective function provides an overall assessment of the algorithm's performance and optimal estimates of its parameter values. We do not claim that the rain gauges represent the true mean-areal rainfall; we merely propose that the rms difference should be as small as possible for high-quality radar rainfall products.

Although research on global optimization has progressed rapidly during the last decade (e.g., Torn and Zilinskas 1989; Rinnooy Kan and Timmer 1989; Duan et al. 1993) there are no reports in the literature on the use of global optimization techniques in radar rainfall calibration. Use of such an approach puts high demand on computational and computer storage resources. To give an example, one month of WSR-88D reflectivity data from Melbourne, Florida, requires approximately 20–30 GB of storage in the archive II format (Crum et al. 1993). Simply reading such volume of data from disk takes several hours on a workstation.

As we mentioned above, the radar–rain gauge difference can not be viewed as radar error. Rain gauge representativeness of the mean-areal rainfall, estimated by radar, decreases as the area size increases. Kitchen and Blackall (1992) showed point to 4 km $\times$ 4 km mean-areal hourly rainfall relative rms differences of the order of 150% for convective storms in England. The rain gauge representativeness error is attributed to two combined effects: the extreme small-scale rainfall variability (Crane 1990) and the large difference in radar–rain gauge sampling resolution (approximately eight orders of magnitude in terms of surface area). These two effects introduce a constant noise in the rms computation that cannot be reduced by any calibration procedure. Assuming the noise is independent from the radar error, when properly quantified, it can be subtracted from the rms calculations to compute the actual radar error (Ciach and Krajewski 1997; Anagnostou et al. 1998b).

4. Global optimization procedure

The high dimensionality of the parameter space and the nonlinear nature of radar rainfall algorithms make the search for the optimal parameters difficult. The PPS has twelve main parameters to be estimated. Another difficulty is the shape of the objective function. The objective function surface can be steep in regions far from the global optimum but it can be relatively flat around the global optimum. The objective function in the multiparameter space is often bumpy and has discontinuous derivatives. There are local optima at different locations of the parameter space, often far from the global optimum. There are also parameter interactions (in the form of elongated ridges and valleys) and nonconvexity of the objective function surface. An important task of this study, therefore, is to select an optimization method that is capable of dealing with these difficulties.

The optimization methods can be classified as deterministic or probabilistic. Deterministic methods provide a guarantee of success only when the objective function satisfies certain restrictions (i.e., continuity, second order differentiability, etc.). Probabilistic methods, on the other hand, do not impose any restrictive conditions on the objective function. We decided to use a probabilistic method because of the nature of the objective function of radar rainfall algorithms and the noisy character of the data.

The method selected is the shuffled complex evolution (SCE-UA) method developed by Duan et al. (1993). The method begins with a population of points randomly selected in the parameter space. The points are partitioned into several communities. The communities grow by random selection of new points, using the simplex geometric shape to direct the search in an improvement direction. Periodically, the entire population is shuffled and the points are assigned to new communities. This process is repeated until the method converges to the global optimum.

5. Data

The data used in this study are from a two-month period, August and September 1995, from central Florida. This dataset was selected as it was part of a NASA experiment referred to as an algorithm intercomparison workshop (AIW). The AIW was conceived by NASA's tropical rainfall measuring mission ground validation team in an effort to select radar rainfall algorithms for satellite-rainfall products validation. Details of this experiment can be found in Krajewski et al. (1996).

The radar data were collected by the KMLB WSR-88D weather radar operated by the NWS and located in Melbourne, Florida. Also, data from 46 rain gauges located within a 200-km range from the radar are used. The rain gauge network is divided into two samples. The first sample is used for calibration of the PPS. The

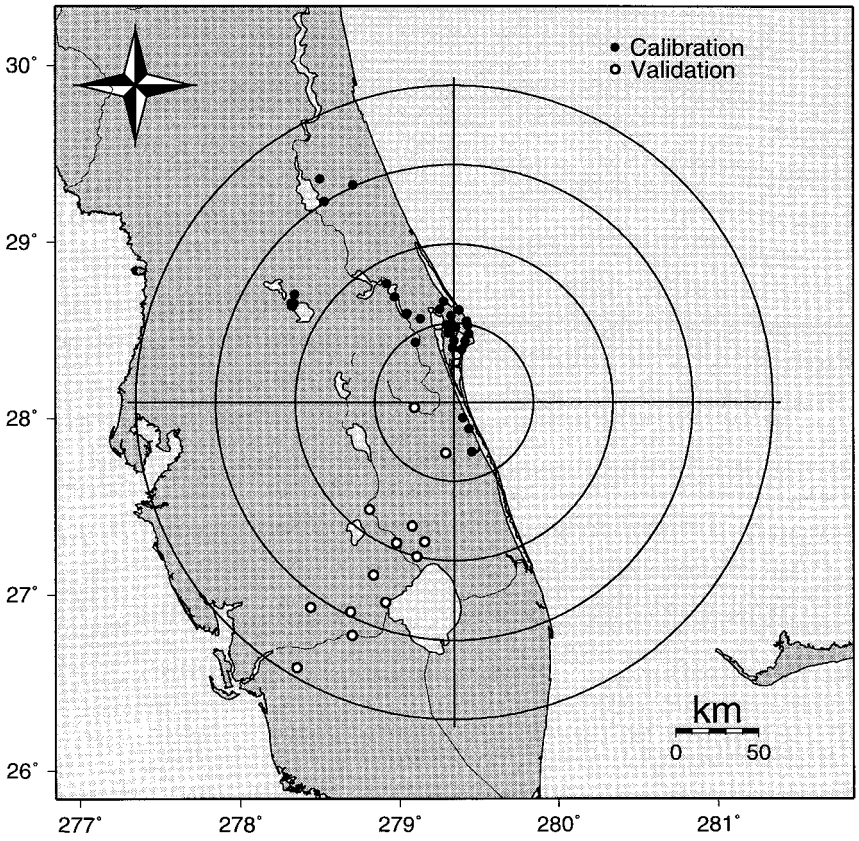

FIG. 1. Florida map, WSR-88D radar coverage (circles correspond to 50-km range intervals), and calibration–validation rain gauge networks.

second sample is used for independent evaluation of the PPS performance. Figure 1 shows a map of Florida, the radar coverage, and the calibration and validation rain-gage locations. The calibration–validation rain gauge network configuration is selected such that the two samples are spatially independent by covering different radar sectors. In this configuration there are 33 calibration rain gauges and 13 validation rain gauges.

To overcome the high demands for computer storage required for two months of WSR-88D (level II) reflectivity data, we used an efficient compression technique. The technique first creates data files containing all the raw reflectivity data that are necessary for the PPS to produce rainfall accumulations at the HRAP grids that correspond to the N_g rain gauge locations (appropriate software is available from the authors). Subsequently, PPS is modified to read the raw radar data from the small files and evaluate the specified objective function [Eq. (2)] over the period of interest (N_p time steps). This compression technique reduces the data storage approximately 1000 times while keeping the data required for calibration unaltered. A similar technique was applied for the calibration of a climatological radar rainfall algorithm by Ciach et al. (1997). To calculate the products of the PPS for the whole radar umbrella, the radar data compression scheme of Kruger and Krajewski (1997) was used. The development of these techniques along with recent advances in computer technologies and storage capacities have made it practically possible and affordable to apply global optimization methods to radar rainfall calibration. Information on the full dataset statistics and radar data quality can be found in Krajewski et al. (1996).

6. Optimization results

The effects of the PPS calibration are investigated by evaluating the reduction in radar–rain gauge rms differences when optimization is applied. The relative reduction in rms is defined as

$$\mathrm{RRMS} = 100 \times \frac{\mathrm{RMS}_{\mathrm{def}} - \mathrm{RMS}_{\mathrm{opt}}}{\mathrm{RMS}_{\mathrm{def}}}, \qquad (3)$$

where RRMS (%) is the relative rms reduction. Here, $\mathrm{RMS}_{\mathrm{def}}$ and $\mathrm{RMS}_{\mathrm{opt}}$ are the rms radar–rain gauge differences of the PPS operating with default and optimal parameters, respectively.

In the calibration of the PPS, the rms was evaluated using rain gauge rainfall rates greater than 0.5 mm h^{-1}. This was done for two reasons: 1) to mitigate the high zero-rain intermittence of rain gauge–rainfall at the 1-h temporal scale, and 2) because a major PPS objective

TABLE 2. Sample size statistics of the calibration ($R_g > 0.5$ mm h^{-1}) and validation ($R_g > 1$ mm h^{-1}) rain gauge networks.

Rain gauge network	Calibration	Validation
Number of gauges	33	13
Hours of rain (at rain gauges)	410	301
Number of radar–gauge pairs	2380	817
Average rain accumulation (mm gauge^{-1})	375.8	323.1

is to perform best during heavy precipitation events. Zero-rain intermittence plays a significant role in radar–rain gauge comparisons as it is a component of rainfall variability. The probability of rainfall detection is quite different for the two sensors. Considering only the rain gauge rainfall over a certain threshold and the corresponding radar rainfall enhances chances for meaningful comparisons.

The validation is done for two different scenarios. In the first scenario all radar and rain gauge pairs were included in the computations of the rms difference (unconditional). In the second scenario only radar and rain gauge pairs with rain gauge hourly rainfall greater than 1.0 mm h^{-1} were included (conditional). This distinction is done to investigate the calibration performance in both the overall and significant precipitation-only events. In Table 2 we present the data statistics for both calibration and validation networks.

The upper and lower bounds defining the parameter space are given in Table 3. Included there also are the optimal parameter values. Most parameters of the PPS converge to values different from the defaults. The significance of using the optimal parameters is shown in Table 4 that summarizes the RRMS validation results for the optimal parameter values listed in Table 3. Results are presented for both August and September, and for the unconditional and conditional scenarios. From Table 4 one can see that overall there is an improvement of about 10%. The table also lists the mean and the coefficient of variation (CV) of the corresponding rain gauge hourly rainfall. The CV is presented to demonstrate the high variability of rainfall within the analyzed period.

We pointed out in section 3 that rainfall variability combined with the radar–rain gauge sampling difference contributes a significant portion of the radar–rain gauge rms difference. Considering that this portion of the rms does not depend on the radar rainfall-estimation procedure, one can understand that the demonstrated rms reduction represents only part of the reduction of the radar-rainfall estimation error. Therefore, the relative rms improvements due to optimization shown in both tables should be viewed as pessimistic. For example, if we assume that the portion of the radar–rain gauge rms difference attributed to sensor sampling differences is between 30% and 75%, which is not a physically unrealistic range for Florida summer rainfall, one can show (see the appendix) that the 10% rms reduction presented above corresponds to a radar rainfall rms error reduction between 15% and 40%, respectively.

TABLE 3. Optimal parameter values derived from the SCE-UA optimization method.

Parameter symbol	Upper limit	Lower limit	Optimal value
Z_{min}	60.0	0.0	60.0
Z_{max}	60.0	0.0	60.0
Z_{tlt}	60.0	0.0	1.0
R_{bi}	230	0	230
j_{CO}	230	0	70.0
CO1	2.0	0.5	1.0
CO2	2.0	0.5	1.0
CO3	0.5	−0.5	−0.046
min (Z to R)	40.0	0.0	5.0
max (Z to R)	60.0	45	51.5
A	—	—	266.5
B	2.0	1.0	1.45

The rms improvement on a day-by-day basis is shown in Fig. 2. Daily mean rain gauge rainfall rate (upper panel), coefficient of variation (middle panel), and the corresponding relative rms (conditional) improvement (lower panel) in the validation sample are presented. Only the days with significant mean rainfall rate are included. Overall the rms reduction is positive and ranging between 2% and 22%. There are days, though, where optimal parameters result in negative RRMS values (increase of the rms difference). The following general observations can be made from Fig. 2: 1) the overall rms reduction is significant (10%); 2) the RMS reduction is high (>8%) during days with significant precipitation; 3) the increase in rms (negative RRMS) is not frequent, is small in magnitude, and is observed during days with small or moderate precipitation. We believe that the second observation is very important and should be given special attention. It shows that PPS optimization improves estimation of heavy precipitation events. This is important because heavy precipitation is mostly responsible for flooding and other rainfall-related hazards.

Figure 3 presents further evidence that optimization improves the PPS performance. The figure shows the radar–rain gauge multiplicative bias defined as

$$\beta_j = \frac{\sum_{t=1}^{N} R_{g_j}(t)}{\sum_{t=1}^{N} R_{r_j}(t)}, \tag{4}$$

TABLE 4. Relative rms reduction in the validation rain gauge sample.

Months	Conditional–unconditional	Rain gauge mean (mm h^{-1})	CV	RRMS (%)
August	All data	0.31	6.5	10.9
	$R_g > 1$ mm h^{-1}	6.16	1.1	10.3
September	All data	0.20	9.5	10.5
	$R_g > 1$ mm h^{-1}	7.53	1.3	11.2

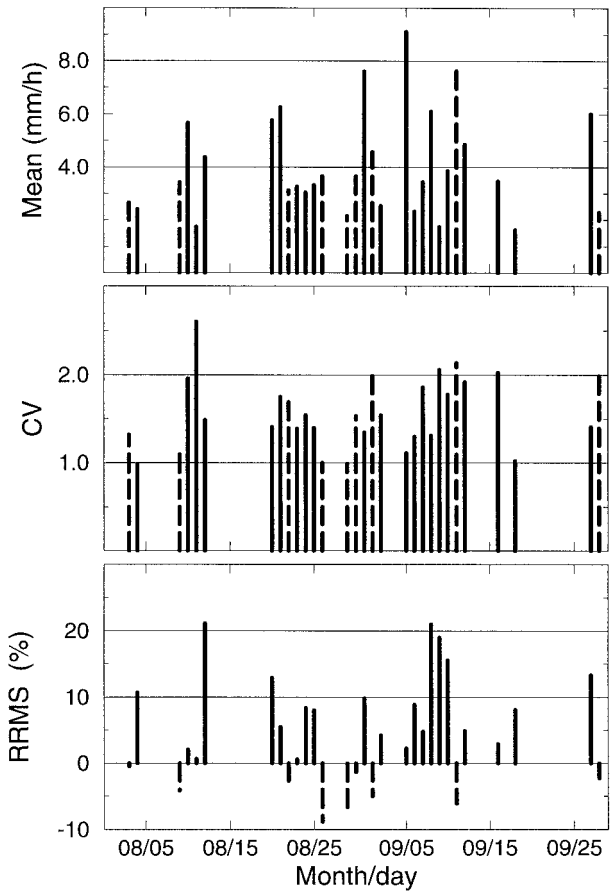

FIG. 2. Relative rms reduction (lower panel) for each day. Upper and middle panels show the mean daily rain gauge rainfall and coefficient of variation, respectively.

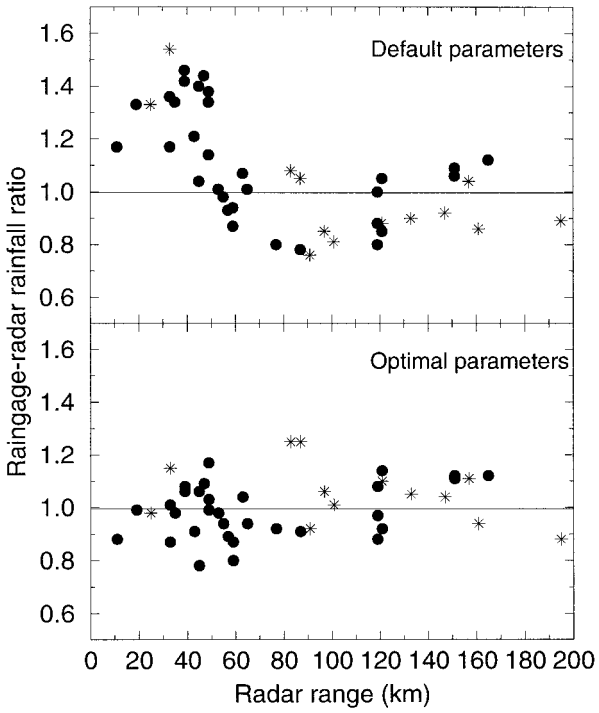

FIG. 3. Ratio of total gauge rainfall over total radar rainfall versus distance of the rain gauge location from the radar. Solid circles and stars correspond to the calibration and validation rain gauges, respectively.

where β is the multiplicative bias, Rg_j and Rr_j represent the rain gauge and radar hourly accumulations at rain gauge location j and hour t, and N is the total number of hours. The bias was calculated using data from both the calibration and validation samples. From Fig. 3 one can see that the PPS range correction formula with parameters estimated by the optimization method significantly reduces (lower panel) the range effect in the uncorrected (upper panel) products.

7. Sensitivity analysis results

Section 6 demonstrated the significance of using optimal parameters, obtained from the global optimization, compared to using default parameters in the PPS. This section shows how sensitive the system is to changes in the optimal parameter values. To demonstrate this, systematic scans in the system's multidimensional parameter space are made. This procedure evaluates the (conditional) rms sensitivity by changing the value of one or simultaneously two parameters and keeping the other parameters at their optimal values. All the presented results are in terms of relative rms difference (with respect to mean rain gauge rainfall).

The first investigated parameter is the minimum reflectivity threshold (min Z to R). This parameter is used by the system to eliminate small reflectivity values that can be due to noise or ground clutter echoes. It should be noted that this parameter has practically no effect on heavy precipitation events, because these events produce relatively high reflectivity values. This is demonstrated in Fig. 4, which shows that the system is practically insensitive to this parameter at values less than 25 dBZ. Note that part of the min Z to R insensitivity is due to the conditioning of the radar–rain gauge rms differences. The dependence significantly increases at reflectivity thresholds greater than 30 dBZ. This means that in the 0–25 dBZ range the reflectivities are too small to contribute significant information to the rms. On the other hand, reflectivity values greater than 25–30 dBZ contain useful quantitative information for rainfall estimation and should not be excluded. The insensitivity of small min Z to R values to the rms criterion is also attributed to the fact that 90% of the total rain volume in this dataset comes from intense small-area convective cells.

Another stage of the PPS is the outlier detection procedure. This procedure has two parameters: 1) $Z_{\max}$ (dBZ), which is the maximum reflectivity beyond which the reflectivities are tested for outliers, and 2) Z_{tlt} (dBZ),

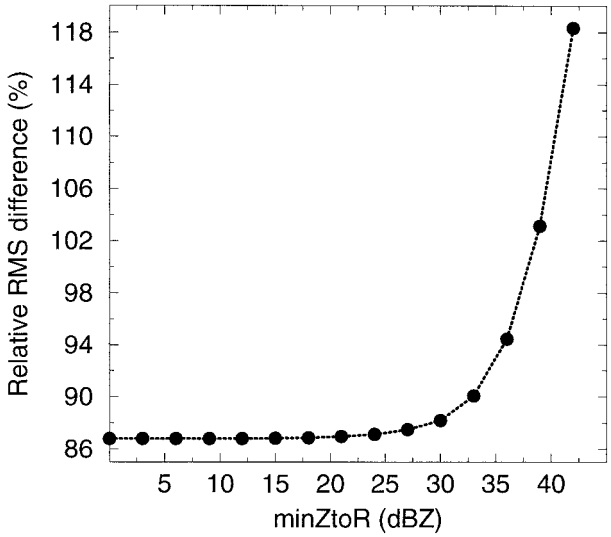

FIG. 4. Minimum reflectivity threshold [min(Z–R)] parameter versus relative rms difference.

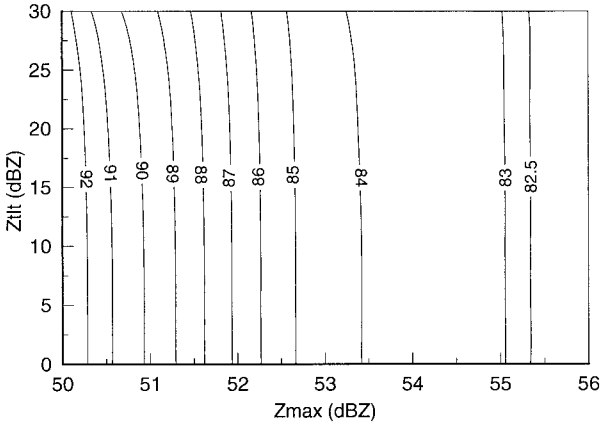

FIG. 5. Rms difference versus outlier detection procedure's Z_{max} and Z_{tlt} parameters. Rms is normalized with respect to mean rain gauge rainfall.

which is the reflectivity assigned to the identified outliers. The contour plot of relative rms versus Z_{max} and Z_{tlt} is shown in Fig. 5. Notice that minimum rms is toward high Z_{max} values and independent of the Z_{tlt} parameter. This shows that the simple single-threshold-based outlier procedure is not improving the system's performance. This is not a surprising result; similar results have been demonstrated in the past (e.g., Krajewski 1987). The corresponding parameters of the minimum rms area of Fig. 5 agree with the estimated parameters from the optimization method.

The next element of the sensitivity analysis is devoted to the biscan maximization. Biscan maximization is a part of PPS's hybrid scan construction strategy. Parameter R_{bi} (range cutoff) defines the range beyond which biscan maximization is applied. Figure 6 shows the rms contours between parameters B (in the Z–R relationship) and the biscan range cutoff. The minimum is toward high-range cutoff values. This indicates that it is better to use the lowest sweep alone rather than the biscan maximization strategy. The gradients of rms surface are strong for B values outside the 1.35–1.6 range. Within the optimum B parameter range (1.35–1.5) the gradients are weaker.

Next we investigate the sensitivity of the system to the exponent B of the nonlinear Z–R transformation. The Z–R parameter A value is adjusted by forcing the overall mean-field radar rain gauge multiplicative bias [Eq. (4)] to become one. Thus, parameter A can be different for different selected parameter sets. This is done to ensure unbiased estimates with minimum radar–rain gauge difference variance. Notice that minimization of the rms difference, used as a sole criterion, does not lead to unbiased estimators. Unbiasedness condition constraints the minimization process. Figure 7 shows the effect of the parameter B on the rms. It is clear that there is a distinct minimum at about 1.45, which is in agreement with the B value found by the global optimization method. This value is nearly identical to the present default value but different from the proposed tropical Z–R parameter value (1.2). The gradient of the RMS close to the minimum is weak but for B values greater than 1.6 or less than 1.35 the gradient becomes stronger.

The next parameter investigated is the maximum reflectivity threshold, max Z to R (dBZ). Figure 8 shows the contours of rms versus B and max Z to R parameter values. Inspection of Fig. 8 indicates that 1) the rms surface is flat along the diagonal, 2) the contours are elongated, and 3) there is no distinct minimum but rather a line of minima along the diagonal. The colinearity shown in Fig. 8 indicates strong dependence between the two parameters. It is clear that when parameter B increases maximum reflectivity threshold should increase accordingly to maintain minimum rms. However, nonexistence of distinct minimum can be explained either as weakness of the single parameter method to dis-

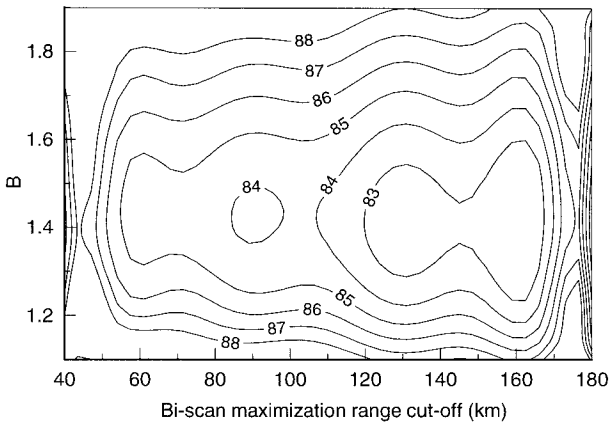

FIG. 6. Rms difference versus biscan maximization's range cutoff parameter and B parameter. Rms is normalized with respect to the mean rain gauge rainfall.

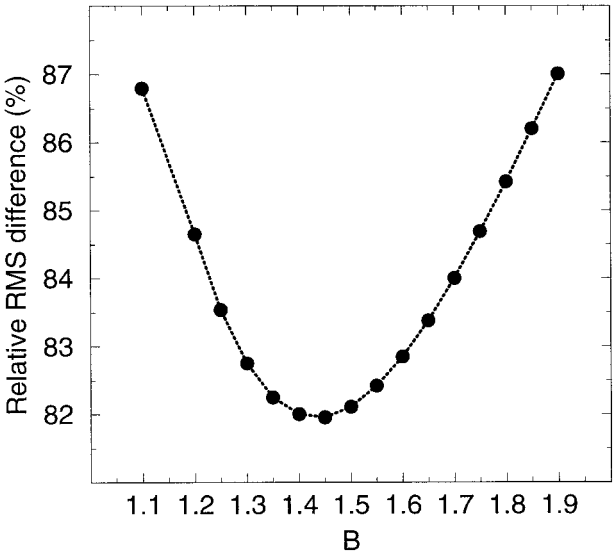

FIG. 7. Rms difference versus *Z–R* relationship's parameter *B*. Rms is normalized with respect to the mean rain gauge rainfall.

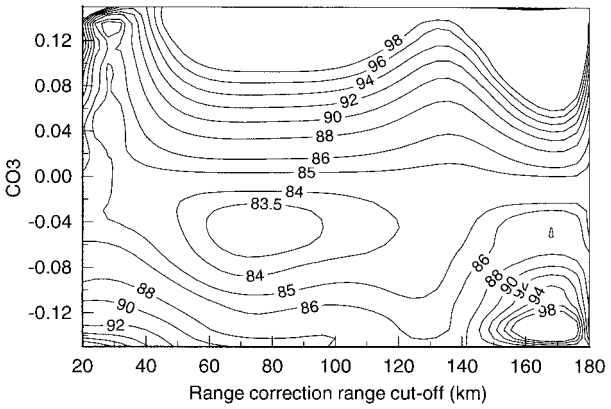

FIG. 9. Rms difference versus range correction formula's range cutoff (j_{co}) and CO3 parameters. Rms is normalized with respect to the mean rain gauge rainfall.

tinguish hail from heavy rain returns or as lack of significant hail effect in the radar rain gauge data used. This can only be investigated using datasets from several hail storm events.

Finally, an important part of the PPS is its range correction formula. The default parameters, CO1 = 1.0, CO2 = 1.0, and CO3 = 0.0, deactivate the formula. Figure 9 shows the contours of relative radar–rain gauge rms difference versus j_{co} and CO3 parameter values. It is clear from the figure that the rms minimum is toward negative CO3 values (−0.04 to −0.07) and a cutoff range between 50 and 80 km. These results are in agreement with the optimal parameters derived from the global optimization method. The parameters corresponding to the minimum rms area shown in Fig. 9 demonstrate that there is a need for range correction in the Next Generation Weather Radar (NEXRAD) products. This observation agrees with results from other studies in the past (e.g., Smith et al. 1996). However, as suggested in Kitchen and Jackson (1993) and reiterated in Hunter (1996), range correction is very difficult to perform when the vertical reflectivity profile is not sampled well, which is the case at long range and stratiform precipitation systems. Our method provides the basis for climatologically testing range correction in the above precipitation estimation scenarios.

The rms sensitivity with respect to parameters CO1 and CO2 is shown in Fig. 10. There is a line of minima passing through point (1.0, 1.0) and along the diagonal with week rms gradients in the vicinity of the minima. The strong colinearity shown in Fig. 10 indicates that there is a redundancy between CO1 and CO2 parameters. The optimal parameter values for CO1 and CO2, derived from the global optimization method, are inside the area of minima shown in Fig. 10.

8. Summary and closing remarks

A global optimization approach is proposed to solve the NEXRAD PPS calibration problem. Optimal param-

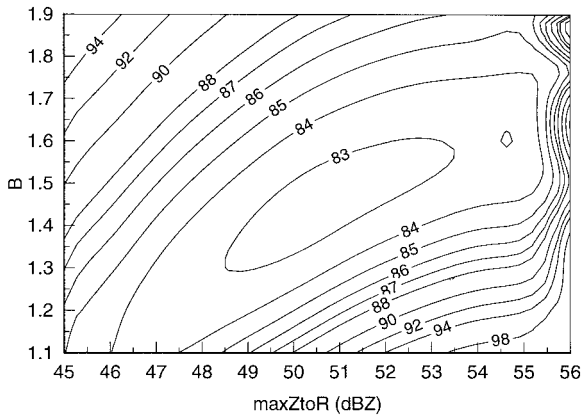

FIG. 8. Rms difference versus maximum reflectivity threshold parameter [max(Z–R)] and *B* parameter. Rms is normalized with respect to the mean rain gauge rainfall.

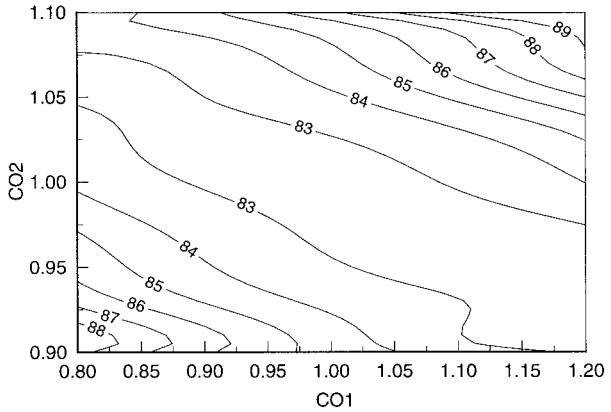

FIG. 10. Relative rms difference versus range correction formula's CO1 and CO2 parameters. Rms is normalized with respect to the mean rain gauge rainfall.

eters are achieved by minimizing the radar–rain gauge rms difference. Rms is evaluated at the final product level, which is 1-h rainfall accumulations at the HRAP grid. The proposed optimization approach is designed to handle difficulties such as high dimensionality of the parameter space, the complexity and highly nonlinear structure of the radar rainfall systems, and the high cost of calculating the objective function (rms difference). A probabilistic global optimization method is used to handle the first three difficulties. A highly efficient compression technique that creates 1000 times smaller size input data has been developed to deal with the last difficulty.

Optimization of the PPS is performed based on two months of WSR-88D radar data from Melbourne, Florida, and the corresponding rain gauge rainfall measurements. The general conclusions from the calibration case study are: 1) overall optimization reduces rms by approximately 10%; 2) in a day-by-day database rms reduction ranges from 2% to 22%, with relatively few cases of negative reduction (increase of rms difference); and 3) rms reduction is significant (>8%) during days of heavy precipitation. Let us note that rainfall during Florida summers probably represents the sternest test of the optimization scheme—showery, spatially inhomogeneous convective precipitation is difficult to sample by rain gauge network. Thus, in other regions where gauge rainfall sampling is better, we expect higher rms error reductions due to an optimized PPS.

A sensitivity analysis was also performed to investigate the significance of the individual parameters on the system's performance. It shows 1) an rms minimum in the multiparameter space exists, 2) the rms surface in the vicinity of the minimum is rather flat, 3) range correction improves NEXRAD rainfall estimates, and 4) the biscan maximization should be deactivated from the system. The last observation confirms empirical experience from WSR-88D sites based on which the biscan maximization has been turned off since 1996. We also note that only a small fraction of total rain corresponds to low rain rates and use of a conditional rms criterion did not allow investigation of the full space of $Z_{\min}$ and min Z to R parameters.

The conclusions of the case study conducted are limited by a data sample of one season for a single site. Other issues regarding the system's parameters such as seasonality effect, stationarity of parameter values, and geographical variations are not investigated. These require much larger datasets from multiple radar sites. Efforts are under way to compile a database of one year of radar data from a Tulsa, Oklahoma, WSR-88D. Also, we have not addressed the problem of a different architecture of the PPS. For example, the system's components such as the hybrid scan construction or the range correction formula could be parameterized in many different ways. The procedure developed in this study could be applied to any radar rainfall algorithm calibration problem.

Acknowledgments. This study was supported by the National Weather Service under the Cooperative Agreement between the Office of Hydrology and the Iowa Institute of Hydraulic Research and by NASA under Grant NAG-5-2094. The authors acknowledge and appreciate useful discussions with James A. Smith, Princeton University, and D.-J. Seo, Office of Hydrology of the National Weather Service. We also thank Anton Kruger, Iowa Institute of Hydraulic Research, for assistance with the radar data, and Stacy R. Stewart, Operational Support Facility, and two anonymous reviewers for their helpful comments on the original manuscript.

APPENDIX

Reduction of RMS Rainfall Estimation Error

As mentioned in section 3, radar–rain gauge differences are due to errors in radar rainfall estimation and sensor sampling differences (hereafter called area-point difference, or APD). Assuming that the two sources of radar–rain gauge difference are uncorrelated and that in the long-term radar and rain gauges have the same mean rainfall [see Ciach and Krajewski (1997) for more details on these assumptions] the following partitioning can be shown for the radar-rain gauge rms difference (2):

$$\mathrm{RMS} = \mathrm{RMS}_{\mathrm{REE}} + \mathrm{RMS}_{\mathrm{APD}}, \qquad \text{(A1)}$$

where subscripts REE and APD stand for rainfall estimation error and area-point difference, respectively. Implementing this rms partitioning into the rms reduction formula (3), after simple derivations one obtains the following expression for the rms rainfall estimation error reduction ($\mathrm{RRMS}_{\mathrm{RRE}}$):

$$\mathrm{RRMS}_{\mathrm{REE}} = \mathrm{RRMS}\left(1 + \frac{\mathrm{RMS}_{\mathrm{APD}}}{\mathrm{RMS}_{\mathrm{REE}}}\right), \qquad \text{(A2)}$$

where RRMS is the reduction of radar–rain gauge RMS difference.

REFERENCES

Ahnert, P., M. Hudlow, E. Johnson, D. Greene, and M. Dias, 1983: Proposed on-site processing system for NEXRAD. Preprints, *21st Conf. on Radar Meteorology*, Edmonton, AB, Canada, Amer. Meteor. Soc., 378–385.

Anagnostou, E. N., W. F. Krajewski, D.-J. Seo, and E. R. Johnson, 1998a: Mean-field radar rainfall bias studies for WSR-88D. *ASCE J. Eng. Hydrol.*, in press.

——, ——, and J. A. Smith, 1998b: Uncertainty quantification of mean-areal radar–rainfall estimates. *J. Atmos. Oceanic Technol.*, in press.

Austin, P. M., 1987: Relation between measured radar reflectivity and surface rainfall. *Mon. Wea. Rev.,* **115,** 1053–1069.

Battan, L. J., 1973: *Radar Observation of the Atmosphere.* The University of Chicago Press, 324 pp.

Ciach, G. J., and W. F. Krajewski, 1997: Error separation in remote sensing rainfall estimation. Preprints, *13th Conf. on Hydrology*, Long Beach, CA, Amer. Meteor. Soc., 137–40.

——, ——, E. N. Anagnostou, M. L. Baeck, J. A. Smith, J. R.

McCollum, and A. Kruger, 1997: Radar rainfall estimation for ground validation studies of the Tropical Rainfall Measuring Mission. *J. Appl. Meteor.,* **36,** 735–747.

Crane, R. K., 1990: Space–time structure of rain rate field. *J. Geophys. Res.*, **95,** 2011–2020.

Crum, T. D., R. L. Alberty, and D. W. Burgess, 1993: Recording, archiving, and using WSR-88D data. *Bull. Amer. Meteor. Soc.*, **74,** 645–653.

Doviak, R. J., and D. S. Zrnic, 1992: *Doppler Radar and Weather Observations.* 2d ed. Academic Press, 562 pp.

Duan, Q., V. K. Gupta, and S. Sorooshian, 1993: A shuffled complex evolution approach for effective and efficient global minimization. *J. Optim. Theory Appl.,* **76,** 501–521.

Fulton, R. A., J. P. Breidenbach, D.-J. Seo, D. A. Miller, and T. O'Bannon, 1998: The WSR-88D rainfall algorithm. *Wea. Forecasting,* **13,** 377–395.

Gan, T. Y., and S. J. Burges, 1990: An assessment of a conceptual rainfall-runoff model's ability to represent the dynamics of small hypothetical catchments. Part 1. Models, model properties, and experimental design. *Water Resour. Res.,* **26,** 1595–1604.

Hendrickson, J. D., S. Sorooshian, and L. Brazil, 1988: Comparison of Newton-type and direct search algorithms for calibration of conceptual rainfall-runoff models. *Water Resour. Res.,* **24,** 691–700.

Hudlow, M. D., 1988: Technological developments in real-time operational hydrologic forecasting in the United States. *J. Hydrol.,* **102,** 69–92.

——, R. Arkell, V. Patterson, P. Pytlowany, and F. Richards, 1979: Calibration and intercomparison of the GATE C-band radars. NOAA Tech. Rep. NESDIS 31, 98 pp.

——, R. K. Farnsworth, and P. R. Ahnert, 1984: NEXRAD technical requirements for precipitation estimation and accompanying economic benefits. HYDRO Tech. Note 4, 49 pp. [Available from Hydraulic Research Laboratory, National Weather Service, Silver Spring, MD 20910.]

Hunter, S. M., 1996: WSR-88D radar rainfall estimation: Capabilities, limitations and potential improvements. *Natl. Wea. Dig.,* **20,** 26–38.

James, W. P., C. G. Robinson, and J. F. Bell, 1993: Radar-assisted real-time flood forecasting. *J. Water Res. Plan. Manag.,* **119,** 32–44.

Kitchen, M., and R. M. Blackall, 1992: Representativeness errors in comparisons between radar and gage measurements of rainfall. *J. Hydrol.,* **134,** 13–33.

——, and ——, 1993: Weather radar performance at long range—simulated and observed. *J. Appl. Meteor.*, **32,** 975–985.

Klazura, G. E., and D. A. Imy, 1993: A description of the initial set of analysis products available from the NEXRAD WSR-88D system. *Bull. Amer. Meteor. Soc.,* **74,** 1293–1311.

Krajewski, W. F., 1987: Radar-rainfall data quality control by the influence function method. *Water Resour. Res.*, **23,** 837–844.

——, and Coauthors, 1996: Radar-rainfall estimation studies for TRMM ground validation. IIHR Tech. Rep. No. 379, 210 pp. [Available from Iowa Institute of Hydraulic Research, University of Iowa, Iowa City, IA 52242.]

Kruger, A., and W. F. Krajewski, 1997: Efficient storage of weather radar data. *Software Practice and Experience,* **27,** 623–635.

National Research Council, 1994: *Estimating Bounds on Extreme Precipitation Events.* National Academic Press, 28 pp.

Rinnooy Kan, A. H. G., and G. T. Timmer, 1989: Global optimization: A survey. *New Methods in Optimization and Their Industrial Uses*, J.-P. Penot, Ed., Birkhauser-Verlag, 189–194.

Smith, J. A., and W. F. Krajewski, 1991: Estimation of the mean field bias of radar rainfall estimates. *J. Appl. Meteor.*, **30,** 397–412.

——, and ——, 1994: Estimation of parameters for the NEXRAD rainfall algorithms. Final Rep., 96 pp. [Available from Hydrologic Research Laboratory, NWS/NOAA, Silver Spring, MD 20910.]

——, G. N. Day, and M. D. Kane, 1992: A statistical framework for long term streamflow forecasting. *J. Water Resour. Plan. Man.*, 82–93.

——, D.-J. Seo, M. L. Baeck, and M. D. Hudlow, 1996: An intercomparison study of NEXRAD precipitation estimates. *Water Resour. Res.*, **32,** 2035–2045.

Torn, A., and A. Zilinskas, 1989: *Global Optimization.* Springer-Verlag, 450 pp.

Zawadzki, I., 1984: Factors affecting the precision of radar measurements of rain. Preprints, *22d Conf. on Radar Meteorology*, Zurich, Switzerland, Amer. Meteor. Soc., 251–256.